



HAL
open science

Non-linear ultrasonic tomography of high-contrasted materials

Régine Guillermin, Philippe Lasaygues

► **To cite this version:**

Régine Guillermin, Philippe Lasaygues. Non-linear ultrasonic tomography of high-contrasted materials. International Congress on Ultrasonics, 2007, Vienne, Austria. CD-ROM(4 p.). hal-00440741

HAL Id: hal-00440741

<https://hal.science/hal-00440741>

Submitted on 11 Dec 2009

HAL is a multi-disciplinary open access archive for the deposit and dissemination of scientific research documents, whether they are published or not. The documents may come from teaching and research institutions in France or abroad, or from public or private research centers.

L'archive ouverte pluridisciplinaire **HAL**, est destinée au dépôt et à la diffusion de documents scientifiques de niveau recherche, publiés ou non, émanant des établissements d'enseignement et de recherche français ou étrangers, des laboratoires publics ou privés.

Non-Linear ultrasonic tomography of high contrast materials

Régine Guillermin, Philippe Lasaygues

Laboratoire de Mécanique et d'Acoustique,
31 chemin Joseph-Aiguier 13402 Marseille cedex 20, guillermin@lma.cnrs-mrs.fr

Abstract This work is concerned with the ultrasonic quantitative imagery of high-contrast 2D target. The non-linear inverse problem is solved via distorted Born iterative procedure involving minimization of discrepancy between measurements and modeling data. Inversions of both simulated and experimental data are presented.

Key words: Ultrasonic tomography, quantitative imagery, high-contrast targets, distorted Born iterative method.

A. Introduction

This study focuses on the ultrasonic characterization and imaging of elastic materials like cylinders or tubes by diffraction tomography technique. In this case, ultrasonic wave propagation is greatly perturbed by the difference in the acoustic impedance between the scatterer and the surrounding medium (soft tissues, water or coupling gel), which results in considerable parasite events such as refraction, attenuation and scattering of waves. The aim of this work is to solve a non-linear inverse scattering problem. Analytical or algebraic approaches may be applied generally involving in a problem of minimization of the differences between modeling data and measurements. Several strategies can be used to model the forward problem and to solve the inverse problem. The Distorted Born Iterative (DBI) method belongs to the class of algebraic reconstruction algorithms and have therefore been investigated in literature ([1]-[7]). Very promising results have been obtained both on synthetic and experimental data especially for electromagnetic inverse diffraction problems [5]-[6], but as far as the authors know few ultrasonic experimental results are available [7]. DBI method was developed to increase the order of application of the Born approximation (valid in the case of weakly contrasted media) to higher orders. Iterations are performed numerically by solving forward and inverse problems at every iteration. This yields quantitative information about the scatterer, such as the speed of sound. Quantitative ultrasonic imaging techniques of this kind are of great potential value in fields such as medicine, underwater acoustics and non-destructive testing.

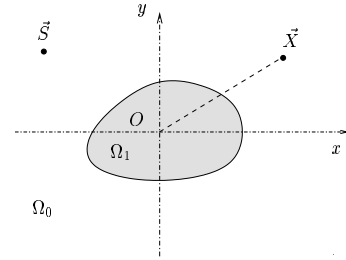


Fig.1. Geometry of the problem

B. Theoretical aspects

Let us consider a cylindrical object of arbitrary cross-section (occupying domain Ω_1 , immersed in a homogeneous infinite medium (occupying domain Ω_0 See Fig.1). Exterior medium Ω_0 is supposed to be fluid-like, linear and isotropic. c_0 et $c_1(\vec{X})$ are the velocities of longitudinal waves respectively in Ω_0 and Ω_1 . Densities of two media are supposed to be constant (i.e. $\rho_1 = \rho_2$). The object is illuminated by a monochromatic line source positioned in \vec{S} : $P^i(\vec{X}, t) = \Re(p^i(\vec{X})e^{-i\omega t})$ with $p^i(\vec{X}) = \frac{i}{4}H_0^{(1)}(k_0\|\vec{X} - \vec{S}\|)$ (with $\omega = 2\pi f$ and $k_0 = \frac{\omega}{c_0}$).

Let us call $p(\vec{X})$ the total pressure field at point \vec{X} . The integral representation of the scattered field $p^s(\vec{X})$ can be written :

$$p^s(\vec{X}) = -k_0^2 \int_{\Omega_1} \Lambda(\vec{X}')p(\vec{X}')G_0(\vec{X}', \vec{X})d\Omega(\vec{X}'), \quad (1)$$

where $G_0(\vec{X}, \vec{X}') = \frac{i}{4}H_0^{(1)}(k_0\|\vec{X} - \vec{X}'\|)$ the free-field Green function and Λ the contrast function of the object :

$$\Lambda(\vec{X}) = 1 - \frac{k^2(\vec{X})}{k_0^2} = 1 - \frac{c_0^2}{c^2(\vec{X})}$$

The integral representation is discretized using moment method. The region of interest D is replaced by a grid of elementary square cells Ω_{pq} , small enough to assume $p(\vec{X})$ and $\Lambda(\vec{X})$ to be constant therein. This leads to the discretized form of (1) :

$$p^s(\vec{X}) = -k_0^2 \sum_{p,q=1}^n \{\Lambda(\vec{X}_{pq})p(\vec{X}_{pq}) \int_{\Omega_{pq}} G_0(\vec{X}, \vec{X}')d\Omega(\vec{X}')\} \quad (2)$$

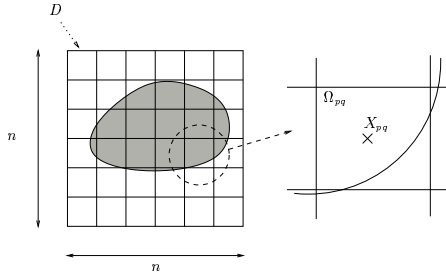


Fig.2. Discretization grid.

Solving the inverse problem consists in finding values of Λ function in domain D . The first-order Born approximation provides a classic linearized solution of this non-linear inverse problem. In this case the total pressure field in the integral term is replaced by the incident field :

$$p^s(\vec{X}) = -k_0^2 \sum_{p,q=1}^n \{ \Lambda(\vec{X}_{pq}) p^i(\vec{X}_{pq}) \int_{\Omega_{pq}} G_0(\vec{X}, \vec{X}') d\Omega(\vec{X}') \} \quad (3)$$

In the inverse problem the scattered field is supposed to be known at M measurements points $\vec{Y}_j; j = 1 \dots M$. Then we generate a system of M linear equation in n^2 unknowns $\Lambda(\vec{X}_{pq}); p, q = 1 \dots n$:

$$p^s(\vec{Y}_j) = -k_0^2 \sum_{p,q=1}^n \{ \Lambda(\vec{X}_{pq}) p^i(\vec{X}_{pq}) \int_{\Omega_{pq}} G_0(\vec{Y}_j, \vec{X}') d\Omega(\vec{X}') \} \quad (4)$$

The inverse problem can be cast in a matrix equation form $P^s = Q\Lambda$, wherein :

$$\Lambda = \begin{bmatrix} \Lambda(\vec{X}_{11}) \\ \vdots \\ \Lambda(\vec{X}_{nn}) \end{bmatrix}, \quad P^s = \begin{bmatrix} p^s(\vec{Y}_1) \\ \vdots \\ p^s(\vec{Y}_M) \end{bmatrix}$$

In general, Q is a non-square ill-conditioned matrix. A mean-squares solution is obtained via conjugate gradient method and Tikhonov regularization [8]. This regularized solution Λ_0 is then used as an initial guess in a DBI algorithm. If the solution Λ_l is supposed to be known for an order l of iteration, the $(l+1)$ -order solution verify [1][2] :

$$p^s(\vec{Y}_j) - p_l^s(\vec{Y}_j) = -k_0^2 \sum_{p,q=1}^n \{ (\Lambda_{l+1}(\vec{X}_{pq}) - \Lambda_l(\vec{X}_{pq})) p_l^i(\vec{X}_{pq}) \int_{\Omega_{pq}} G_l(\vec{Y}_j, \vec{X}') d\Omega(\vec{X}') \} \quad (5)$$

where G_l is the inhomogeneous Green function for an object Λ_l immersed in Ω_0 . Then $G_l(\vec{Y}_j, \vec{X})$ is the total pressure field calculated at point \vec{Y}_j for a line source placed

at \vec{X} illuminating an object with characteristic function Λ_l immersed in Ω_0 .

p_l et p_l^s are the total and scattered pressure field for the same object illuminated by a line source placed at point \vec{S} . These quantities are evaluated solving a forward integral problem (1). A condensed form of the DBI procedure can be written (more details can be found in [9]) :

$$\begin{cases} P_0 = P^i \\ P^s = Q_0(P_0)\Lambda_0 \\ \\ P_l = [\Gamma(\Lambda_l)]^{-1}P^i \\ P^s - P_l^s = Q_l(P_l)[\Lambda_{l+1} - \Lambda_l] \end{cases} \quad (6)$$

C. Numerical study

We give here the results of inversion with DBI algorithm for numerical simulations. The test zone D is a square $2cm \times 2cm$, composed of 60×60 pixels. Simulated data are obtained via boundary integral equations method. The chosen target is described in Fig. 3 and corresponds to the object used in the experimental study. It was a non-circular homogeneous isotropic shell made of artificial resin. The density of the resin was $\rho_1 = 1150kg/m^3$, and the mean velocity of the compressional wave was $c_1 = 2400m/s$. The surrounding fluid-like medium (and the hollow area) was water at a temperature of 18° ($\rho_0 = 1000kg/m^3, c_0 = 1480m/s$). Even if, in experimental study, a contrast of density exists between target and surrounding medium, for numerical simulations we have chosen $\rho_1 = \rho_0 = 1000kg/m^3$.

Transmitter and receiver describe a circle of radius $17cm$ all around the object, with an angular increment of 5° for the transmitter and 10° for the receiver.

Five frequencies were used for the simulations: 150 kHz, 180 kHz, 250kHz, 300 kHz and 350 kHz. Results are shown in Fig.4.

The initial frequency was chosen so that the first-order Born solution does not include any artifacts. Previous studies [2],[4] have shown that if the phase shift resulting from the presence of the scatterer is greater than π , the reconstruction will present important artifacts. We therefore chose a frequency such as $f < \frac{c_0 c_1}{2d|c_1 - c_0|} \sim 140kHz$ (where d is the largest dimension of the scatterer). The initial solution is given by the first-order Born estimate. At each frequency, the initial solution was the final result of the iterations performed at the previous frequency. Fig.4 displays results of the DBI inversion of simulated data. Final result was found to be satisfactory on the qualitative level (as regards the shape, dimensions, and location). From the quantitative point of view (velocity measurements) results are of good quality too, but it is important to notice that the final value of the reconstructed velocity strongly depends on the regularization parameter used for the mean-squares inversion procedure. A study for the optimization of this parameter is now in progress [10].

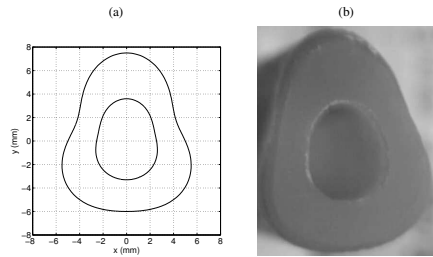


Fig.3. Chosen target : (a) for the numerical study, (b) for the experimental study.

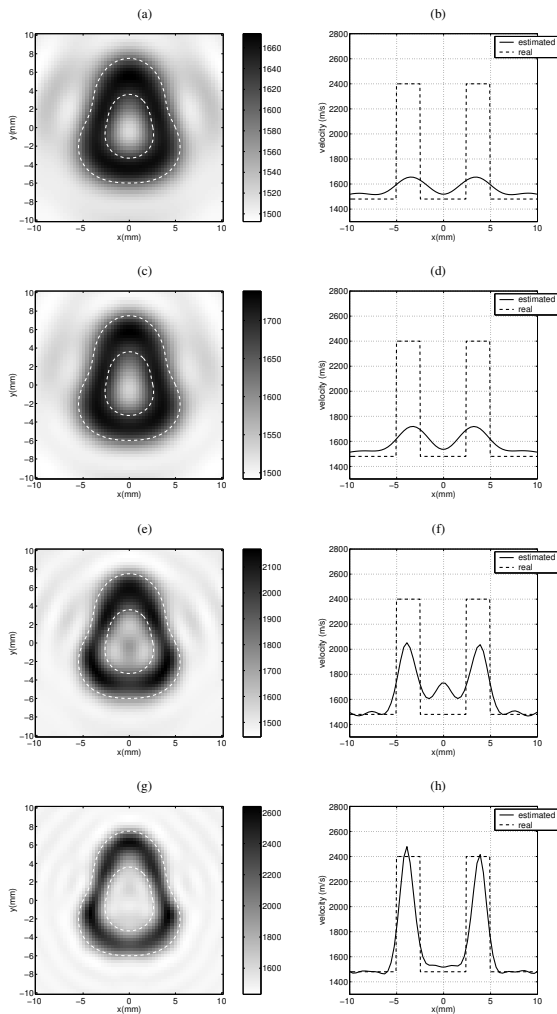


Fig.4. Ultrasonic distorted Born iterative inversion of simulated data, left: tomograms 60 x 60 pixels, right: x-pixel profiles drawn at $y = 0$ mm; (a-b) 9 iterations at 150 kHz; (c-d) 4 iterations at 180 kHz; (e-f) 25 iterations at 250 kHz; (g-h) 10 iterations at 300 kHz + 24 iterations at 350 kHz

D. Experimental study

D.1. Experimental set-up

The experimental setup used here was designed for performing diffraction measurements. Stepping motors insure precise rotations of the transmitter and the receiver.

Ultrasounds were generated by a pulse receiver device and piezo-composite wide-band transducers (whose central frequency was 0.25 MHz and the usable bandwidth was approximately from 135 to 375 kHz). The object was placed in the center of the measuring system. Ultrasonic measurements were performed in water at room temperature. Configuration of acquisitions is described in Fig.5. Transmitter rotated all around the target with an angular increment of 5° (72 emission positions). Receiver rotated from 40° to 320° respect to the transmitter position with an angular increment of 10° (29 reception positions for every emission). Received signals were digitized (8 bits, 20 MHz) using an oscilloscope, stored (4000 samples) on a computer via a General Purpose Interface Bus for off-line analysis. An example of transmitted signal and its spectrum is given on Fig.6.

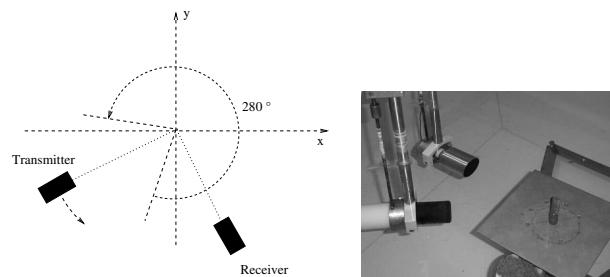


Fig.5. Configuration of acquisitions

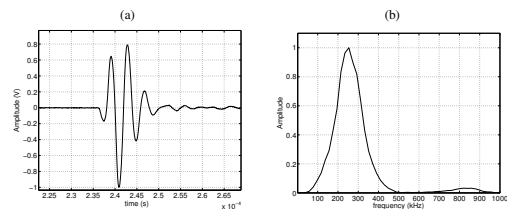


Fig.6. Example of transmitted signal (a) temporal signal, (b) spectrum

D.2. Experimental results

Fig.7 displays images reconstructed via DBI inversion method. First it is important to notice that in our experimental data, contrast of density exists between the target and the surrounding medium that is not taken into account in the inversion scheme. For this kind of resin, density contrast is quite small and can be considered as additional noise on experimental data. Moreover, it is very difficult to find a high-contrast material of same density than water, the chosen resin offers the best compromise the authors can find. It can be seen here that the resolution and the quality of the modeled contrast improved gradually, as with the inversion of the numerical data (Fig.4). As in the case of the simulations, the geometry was fairly accurate, whereas the velocity was less accurately estimated, with a relative

error of about 10% in some areas. This was mainly due to the regularization parameter selected. cedure.

F. Literature

- [1] W. C. Chew, *Waves and fields in Inhomogeneous Media*, IEEE PRESS, New York, 1995
- [2] O.S. Haddadin and E. S. Ebbini : Multiple frequency distorted Born iterative method for tomographic imaging, *Acoustical Imaging* **23**, Plenum Press, 1997
- [3] O.S. Haddadin and E. S. Ebbini : Imaging strongly scattering media using a multiple frequency distorted Born iterative method, *IEEE transactions on Ultrasonics , Ferroelectrics and Frequency Control*, **45**, 1485-1496, 1998
- [4] O.S. Haddadin : *Ultrasound inverse scattering for tomographic imaging and self-focusing arrays*, PhD Thesis, University of Michigan, 1998
- [5] A. G. Tijhuis, K. belkebir, A. C. S. Litman and B. P. de Hon : Multiple-frequency distorted-wave Born approach to 2D inverse profiling, *Inverse Problems* **17**, 1635-1644, 2001
- [6] K. Belkebir and M. Saillard : Special section : Testing inversion algorithms against experimental data, *Inverse Problems* **17**, 1565-1571, 2001
- [7] C. Lu, J. Lin, W. Chew and G. Otto : Image reconstruction with acoustic measurement using distorted Born iteration method, *Ultrasonic Imaging* **18** 2, 140-156, 1996
- [8] A.N. Tikhonov, A.V. Goncharsky, V.V.Stepanov and A.G. Yagola : *Numerical method for the solution of ill-posed problems*, Kluwer Academic Publishers, Dordrecht, 1995.
- [9] P. Lasaygues, R. Guillermin and J-P. Lefebvre : Distorted Born Diffraction Tomography Applied to Inverting ultrasonic Field Scattered by Noncircular Infinite Elastic Tube, *Ultrasonic Imaging* **28**, 211-229, 2006.
- [10] P.C. Hansen : Analysis of discrete ill-posed problems by mean of the L-curve, *SIAM Rev.* **34**, 561-580, 1992
- [11] P. Charbonnier, L. Blanc-Féraud, G. Aubert and M. Barlaud, Deterministic edge-preserving regularization in computed imaging, *IEEE Trans. Image Process.* **6** (2), 298-311, 1997.

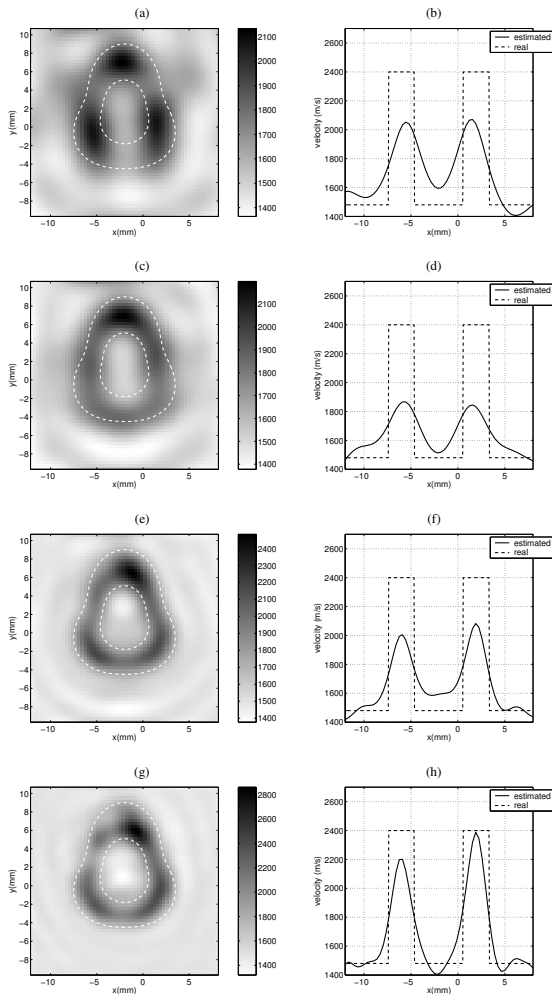


Fig.7. Ultrasonic distorted Born iterative inversion of experimental data, left: tomograms 60 x 60 pixels, right: x-pixel profiles drawn at $y = 0$ mm; (a-b) 11 iterations at 150 kHz; (c-d) 9 iterations at 180 kHz; (e-f) 14 iterations at 250 kHz; (g-h) 13 iterations at 300 kHz + 11 iterations at 350 kHz

E. Conclusion

This paper deals with the two-dimensional imaging of a high-contrast target using distorted Born iterative tomography. Examples given in this paper involve a non-canonical homogeneous shape, and results were based on numerical simulations and experiments. Results obtained here are very promising because the geometrical and physical parameters of the scatterer were accurately reconstructed. Various way of improving this method will now be investigated. One important aspect of the inversion scheme is the choice of regularization procedure. In this paper, Tikhonov regularization method was employed and work is in progress on how to choose the regularization parameter. Another drawback of the DBI algorithm is the density-constant hypothesis. Complementary works must be done to take density contrast into account in the inversion pro-